ISSN 1674-1056
http://cpb.iphy.ac.cn
http://iopscience.iop.org/cpb
中国物理 B
Chinese Physics
中国物理 Chinese Physics B

Electronic, optical property and carrier mobility of graphene, black phosphorus, and molybdenum disulfide based on the first principles

Congcong Wang(王聪聪), Xuesheng Liu(刘学胜), Zhiyong Wang(王智勇), Ming Zhao(赵明), Huan He(何欢), Jiyue Zou(邹吉跃)

Citation: Chin. Phys. B . 2018, 27(11): 118106. **doi:** 10.1088/1674-1056/27/11/118106
Journal homepage: http://cpb.iphy.ac.cn; http://iopscience.iop.org/cpb

What follows is a list of articles you may be interested in

Dynamically tunable terahertz passband filter based on metamaterials integrated with a graphene middle layer

MaoSheng Yang(杨茂生), LanJu Liang(梁兰菊), DeQuan Wei(韦德泉), Zhang Zhang(张璋), Xin Yan(闫昕), Meng Wang(王猛), JianQuan Yao(姚建铨)

Chin. Phys. B . 2018, 27(9): 098101. **doi:** 10.1088/1674-1056/27/9/098101

Novel graphene enhancement nanolaser based on hybrid plasmonic waveguides at optical communication wavelength

Zhengjie Xu(徐政杰), Jun Zhu(朱君), Wenju Xu(徐汶菊), Deli Fu(傅得立), Cong Hu(胡聪), Frank Jiang

Chin. Phys. B . 2018, 27(8): 088104. **doi:** 10.1088/1674-1056/27/8/088104

Modulated thermal transport for flexural and in-plane phonons in double-stub graphene nanoribbons

Chang-Ning Pan(潘长宁), Meng-Qiu Long(龙孟秋), Jun He(何军)

Chin. Phys. B . 2018, 27(8): 088101. **doi:** 10.1088/1674-1056/27/8/088101

Free-standing, curled and partially reduced graphene oxide network as sulfur host for high-performance lithium-sulfur batteries

Hui-Liang Chen(陈辉亮), Zhuo-Jian Xiao(肖卓建), Nan Zhang(张楠), Shi-Qi Xiao(肖仕奇), Xiao-Gang Xia(夏晓刚), Wei Xi(席薇), Yan-Chun Wang(王艳春), Wei-Ya Zhou(周维亚), Si-Shen Xie(解思深)

Chin. Phys. B . 2018, 27(6): 068101. **doi:** 10.1088/1674-1056/27/6/068101

Facilitative effect of graphene quantum dots in MoS_2 growth process by chemical vapor deposition

Lu Zhang(张璐), Yongsheng Wang(王永生), Yanfang Dong(董艳芳), Xuan Zhao(赵宣), Chen Fu(付晨), Dawei He(何大伟)

Chin. Phys. B . 2018, 27(1): 018101. **doi:** 10.1088/1674-1056/27/1/018101

Electronic, optical property and carrier mobility of graphene, black phosphorus, and molybdenum disulfide based on the first principles*

Congcong Wang(王聪聪), Xuesheng Liu(刘学胜)†, Zhiyong Wang(王智勇), Ming Zhao(赵明), Huan He(何欢), and Jiyue Zou(邹吉跃)

Beijing University of Technology, Institute of Laser Engineering, Beijing 100124, *China*

(Received 22 July 2018; revised manuscript received 30 August 2018; published online 25 October 2018)

The band structure, density of states, optical properties, carrier mobility, and loss function of graphene, black phosphorus (BP), and molybdenum disulfide (MoS_2) were investigated by the first-principles method with the generalized-gradient approximation. The graphene was a zero-band-gap semiconductor. The band gaps of BP and MoS_2 were strongly dependent on the number of layers. The relationships between layers and band gap were built to predict the band gap of few-layer BP and MoS_2. The absorption showed an explicit anisotropy for light polarized in (1 0 0) and (0 0 1) directions of graphene, BP, and MoS_2. This behavior may be readily detected in spectroscopic measurements and exploited for optoelectronic applications. Moreover, graphene (5.27×10^4 $cm^2\cdot V^{-1}\cdot s^{-1}$), BP ($1.5\times10^4$ $cm^2\cdot V^{-1}\cdot s^{-1}$), and MoS_2 (2.57×10^2 $cm^2\cdot V^{-1}\cdot s^{-1}$) have high carrier mobility. These results show that graphene, BP, and MoS_2 are promising candidates for future electronic applications.

Keywords: graphene, two-dimensional (2D) materials, band structure, black phosphorus

PACS: 81.05.ue, 71.15.Mb, 73.20.At **DOI:** 10.1088/1674-1056/27/11/118106

1. Introduction

Van der Waals crystals, including graphene, black phosphorus (BP), and transition-metal dichalcogenide nanomaterials that can be described as MX_2 (M = Mo, W, Nb, Ta, Ti, Zr, Hf, Re; X = S, Se), are currently under intensive research, driven by the wide potential application in high performance optoelectronic devices, such as a field-effect transistor (FET). They can be used in passively mode-locked and passively Q-switched fiber laser or solid laser as the saturable absorber. Graphene, BP, and MoS_2 have the advantages of a moderate electronic band gap, a reasonably high carrier mobility, and excellent electrode–channel contacts because of the layer-controllable crystal structure. Graphene is a gapless semiconductor with the advantage of high carrier mobility due to its very low carrier effective mass.[1] However, the application of graphene in semiconductor materials is limited, also because of the zero-band gap. For this reason, the emergence of few-layer BP has attracted much attention. Few-layer BP has advantages of high mobility, high in-plane anisotropy, a moderate band gap (0.3–1.5 eV), and linear dichroism.[2] It can be widely used in optical detection and communications. BP is an intrinsic p-type semiconductor, which is different from graphene and MoS_2.[3] Compared with graphene and BP, MoS_2 has more application value in hydrogen adsorption and storage due to a band gap of 1.3–1.8 eV.

It is difficult to measure the band gaps of few-layer graphene, BP, and MoS_2 experimentally. To guide the experimental study, the electronic structure of graphene, BP, and MoS_2 were calculated using the generalized gradient approximation (GGA) based on the density functional theory (DFT). Rudenko *et al.*, Cai *et al.*, and Qiao *et al.* calculated the properties of BP from monolayer to five-layer.[1,2,4] Wang *et al.*, Hu *et al.*, and Phuc *et al.* calculated the properties of MoS_2.[5–7] Although the band and the lattice structures of few-layer graphene, BP, and MoS_2 have been extensively studied, detailed research on optical properties is rarely reported. The loss function represents the energy loss of the electrons quickly through material and electron excitation in the interior or surface of the material.[8] Very few researchers have studied this aspect. In addition, most of these studies were independent, a comparative and comprehensive study on few-layer graphene, BP, and MoS_2 has not yet emerged.

In this paper, a first-principles calculation theory was used to study the structural properties, energy gap, the density of states (DOS), the partial density of states (PDOS), optical properties, carrier mobility, and loss function of few-layer graphene, BP, and MoS_2. To predict the band gap of few-layer BP and MoS_2, the relationships between the number of layers and the band gap were built. In addition, the absorption and carrier mobility were analyzed in detail.

2. Calculation method

All of the models were built and optimized with the CASTEP module, with the generalized-gradient approximation (GGA) of the exchange–correlation functional (RPBE). The cutoff energy for the plane wave was set to 400 eV. The

*Project supported by the National Key R&D Program of China (Grant No. 2017YFB0305800).

†Corresponding author. E-mail: liuxuesheng@bjut.edu.cn

© 2018 Chinese Physical Society and IOP Publishing Ltd

convergence tolerance of force on each atom during structure relaxation was reduced to less than 0.03 eV/Å. The maximal displacement of atoms was reduced to less than 1×10^{-3} Å. The total energy variation of the system was reduced to less than 2.0×10^{-6} eV/atom. The internal stress between atoms was reduced to less than 0.05 GPa. The SCF tolerance was reduced to less than 1.0×10^{-6} eV/atom. The Brillouin zone integration was performed with $50 \times 50 \times 1$ k-points for graphene, BP, and MoS_2. To improve the speed of this calculation, we used higher symmetry k points in BP and MoS_2 calculation. The vacuum distance of 20 Å was used in order to isolate the slabs from their periodic images, for graphene, BP, and MoS_2 from monolayer to five-layer.[9]

3. Results and discussion

3.1. Structural properties

Figure 1 shows the crystal structures of graphene, BP, and MoS_2. Table 1 lists the optimized lattice constants (a, b, c) of graphene, BP, and MoS_2. The d is the height of each layer. The monolayer graphene has a two-dimensional (2D) periodic honeycomb structure composed of six-member carbon rings with sp^2 hybridization. The carbon–carbon bond length in graphene is 1.424 Å. Few-layer graphene is interlinked by van der Waals force.

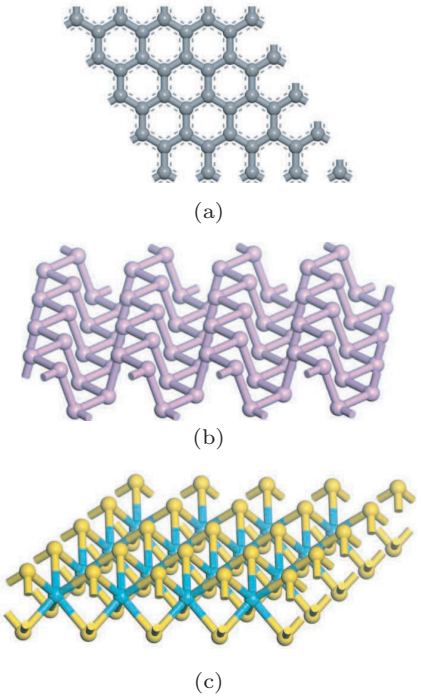


Fig. 1. (color online) The crystal structures of (a) grapheme, (b) BP, (c) MoS_2.

Bulk BP is an orthorhombic crystal with the *Cmca* space group. The puckered layer is composed of zigzag direction and armchair direction. Based on bulk BP, the structures of monolayer and few-layer phosphorene were obtained by mechanical exfoliation.[16] The monolayer BP has a puckered honeycomb structure in which a phosphorus atom covalently bonds with three adjacent atoms.[17] Due to the lone pairs electrons associated with each atom, the sp^3 hybridization is formed by two P atoms with three bonding orbitals.[4,18] The lattice parameter a increases and b decreases from monolayer to five-layer BP. There is an abrupt reduction of a from the monolayer to the bilayer due to the interlayer interactions in the bilayer.[1] Few-layer MoS_2 has the S/Mo/S sandwich structure, interlinked by van der Waals force. In contrast from BP, the lattice parameters of MoS_2 barely change from monolayer to five-layer. The calculated geometric structures are in good agreement with the previous theoretical and experimental results. Therefore, the theoretical calculation is correct.

Table 1. Lattice constants of graphene, BP, and MoS_2.

		Graphene		
		a/Å	b/Å	c/d/Å
Graphene	monolayer (this work)	2.445	–	–
	monolayer[10]	2.461	–	–
	monolayer[11]	2.46	–	–
BP	bulk (this work)	3.294	10.686	4.409
	bulk[12]	3.325	10.429	4.398
	bulk[13]	3.313	10.473	4.374
	monolayer	3.267	4.802	3.034
	monolayer[1]	3.33	4.58	3.20
	bilayer	3.273	4.755	3.025
	bilayer[1]	3.33	4.52	3.20
	three-layer	3.283	4.743	3.024
	three-layer[1]	3.33	4.51	3.20
	four-layer	3.290	4.653	3.025
	four-layer[1]	3.34	4.50	3.20
	five-layer	3.275	4.736	3.035
	five-layer[1]	3.34	4.49	3.20
MoS_2	bulk (this work)	3.15	3.15	12.14
	bulk[14]	3.13	3.13	11.89
	monolayer (this work)	3.189	3.189	3.118
	monolayer[5]	3.166	3.166	3.170
	monolayer[15]	3.17	3.17	3.119
	bilayer	3.190	3.190	3.118
	three-layer	3.191	3.191	3.119
	four-layer	3.190	3.190	3.119
	five-layer	3.190	3.190	3.120

3.2. Band gaps analysis

Figure 2 shows the band gaps of monolayer graphene, BP, and MoS_2. Brillouin zone path of graphene primitive cell is G (0 0 0) → K (0.333 0.667 0) → F (0 0.5 0) → G (0 0 0). Brillouin zone path of BP primitive cell is G (0 0 0) → Z (0 0 0.5) → T (−0.5 0 0.5) → Y (−0.5 0 0) → S (−0.5 0.5 0) → X (0 0.5 0) → U (0 0.5 0.5) → R (−0.5 0.5 0.5). Brillouin zone path of MoS_2 primitive cell is G (0 0 0) → A (0 0 0.5) → H (−0.333 0.667 0.5) → K (−0.333 0.667 0) → G (0 0 0) → M (0 0.5 0) → L (0 0.5 0.5) → H (−0.333 0.667 0.5). The graphene is a zero-band-gap semiconductor. Monolayer graphene film's conduction band and valence band appear conical and meet in

a Dirac point. The calculated band structure of monolayer BP shows a direct band gap of 1.227 eV at the X point. The bulk MoS_2 is an indirect band gap semiconductor. The edge positions of the valence band and conduction band change from bulk MoS_2 to monolayer MoS_2.[19] MoS_2 becomes a direct band gap semiconductor with the decreased number of layers. The calculated band structure of monolayer MoS_2 shows a direct band gap of 1.806 eV at the K point. The calculated band gaps are in good agreement with the previous theoretical results.

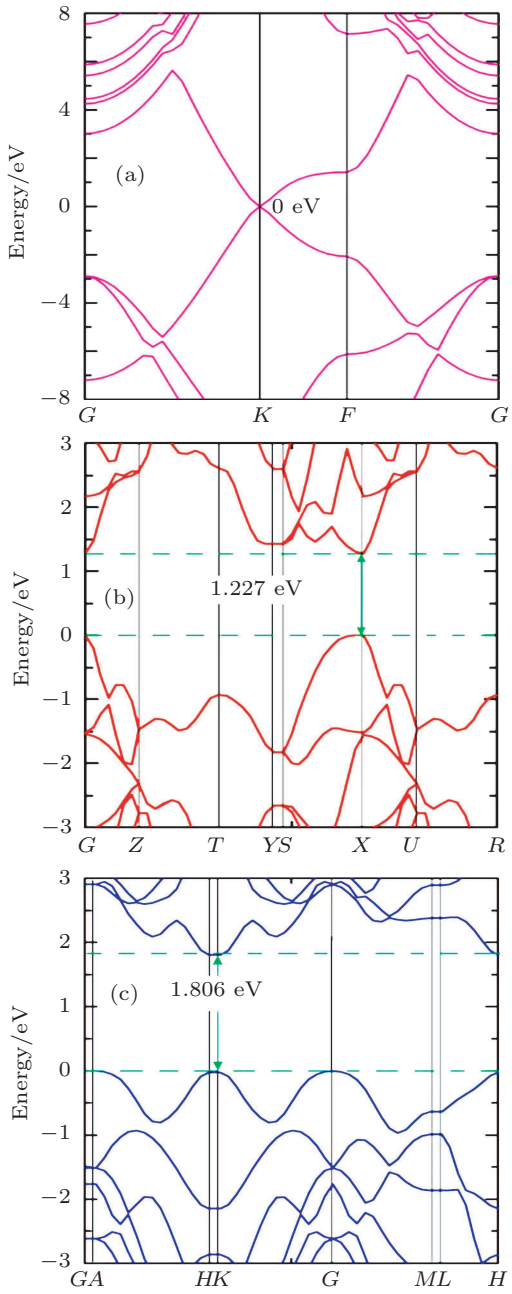


Fig. 2. (color online) The band gaps of monolayer materials: (a) graphene, (b) BP, and (c) MoS_2.

Figure 3 shows the relationships between layers and band gaps of BP and MoS_2. The band gaps are strongly dependent on the number of layers. When the number of layers increases, the band gaps decrease. The band gap can be adjusted by changing the layers of Van der Waals crystals. The relationships between layers and band gaps of BP and MoS_2 meet the exponential correlation on the whole; that is,

$$E_g = E_0 + A\,e^{\alpha N}, \tag{1}$$

where E_g is the band gap, E_0 is the band gaps for bulk BP and MoS_2, which are calculated to be 0.37 eV and 0.68 eV, respectively, and N is the number of layers. The fitting parameters A and α are 1.39 and -0.48 for BP, and 1.53 and -0.30 for MoS_2. The R-squares of the fitting curve are all above 99.99%. The equation is based on the PBE function, it has errors between experimental values and calculated results. However, it still has theoretical guidance.

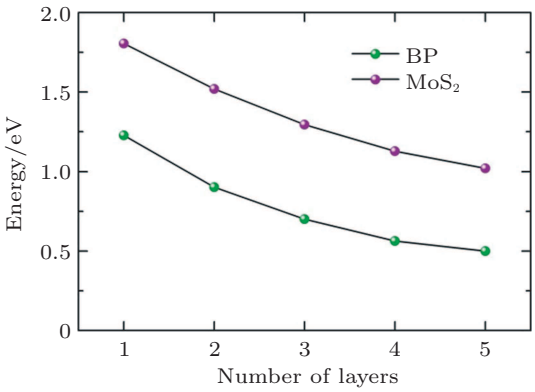


Fig. 3. (color online) The relationships between layers and band gaps.

3.3. DOS and PDOS analysis

Figure 4 shows the DOS and PDOS of monolayer graphene, BP, and MoS_2. The green dotted line displays the Fermi level. Because the conduction band minimum (CBM) and the valence band maximum (VBM) of graphene are both determined by C (p) orbit, the band gap of graphene is determined by C (p) orbit. As the CBM and VBM are both determined by P (p) orbit, the band gap of BP is determined by P (p) orbit. The CBM of the monolayer MoS_2 is determined by the Mo (d) orbit, while the VBM of the monolayer MoS_2 is determined by a hybridization of the S (p) orbit and the Mo (d) orbit.

3.4. Absorption spectra analysis

Figure 5 shows the absorption spectra of graphene, BP, and MoS_2. The absorption shows an explicit anisotropy for light polarized in (1 0 0) and (0 0 1) directions. The (1 0 0) direction is the direction of the stretching area of 2D material. The (0 0 1) direction is the direction of layers increasing. This behavior may be readily detected in spectroscopic measurements and exploited for optoelectronic applications.

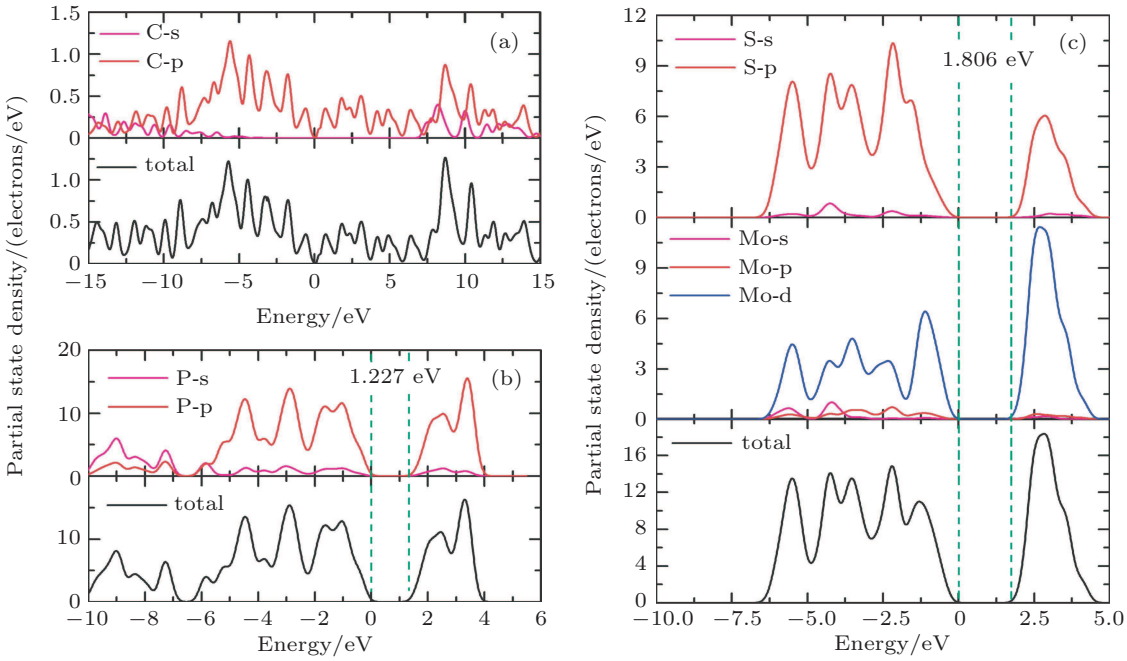


Fig. 4. (color online) The DOS and PDOS of monolayer materials: (a) graphene, (b) BP, and (c) MoS_2.

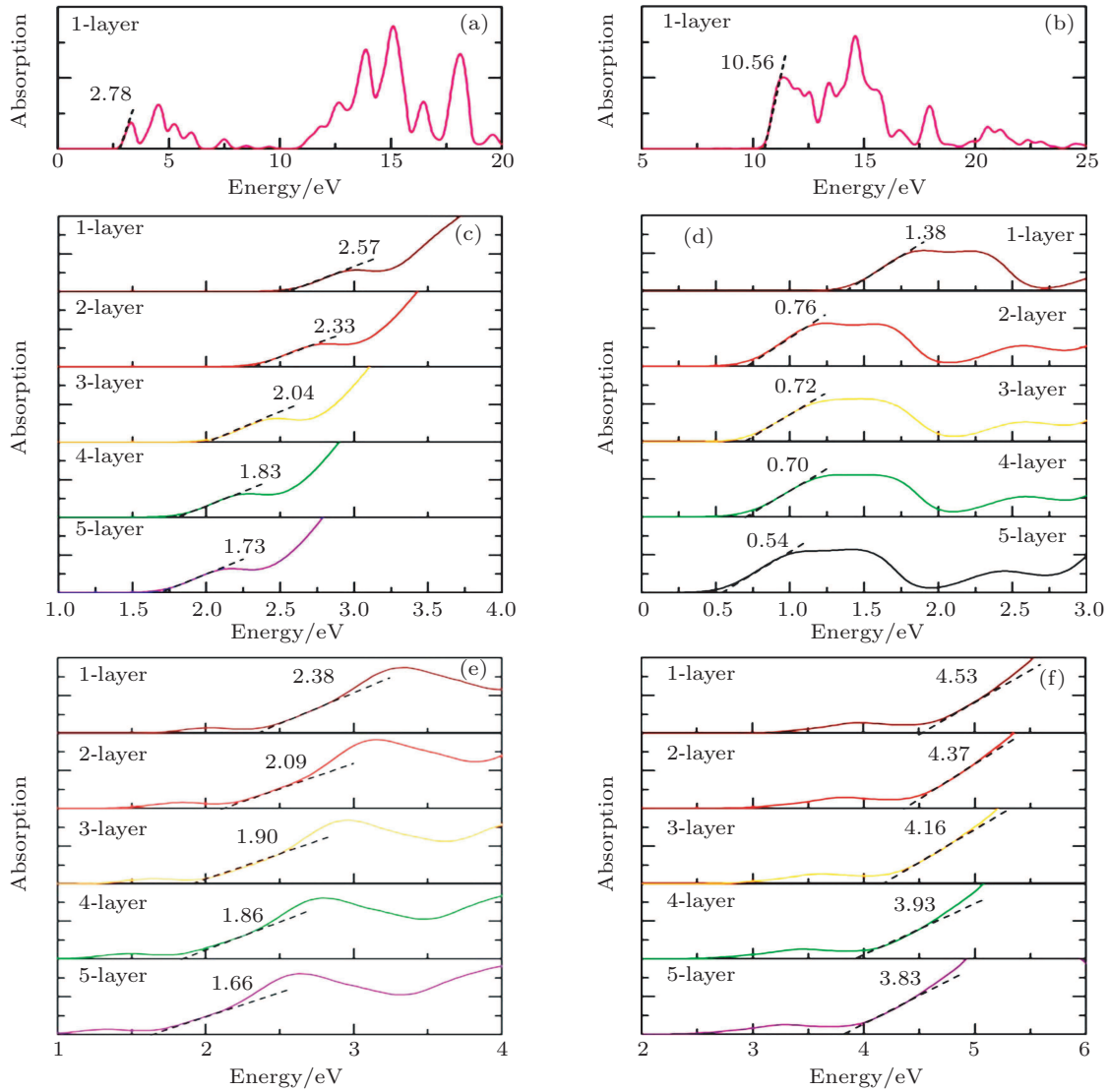


Fig. 5. (color online) The absorption spectra of (a) (1 0 0) graphene, (b) (0 0 1) graphene, (c) (1 0 0) BP, (d) (0 0 1) BP, (e) (1 0 0) MoS_2, and (f) (0 0 1) MoS_2.

Among graphene, BP, and MoS_2, graphene has the highest absorption threshold. The absorption and transmission of monolayer graphene are 2.3% and 97.7%, respectively.[20] Therefore, it can be widely used in solar cell and liquid crystal device window layer field. The absorption threshold of BP is lower than that of MoS_2, because of the smaller band gap. Given the band gap variations, the absorption thresholds of BP and MoS_2 are decreased from monolayer to five-layer. We can determine the sample orientation using the linear dichroism of BP and MoS_2 easily. Once the sample orientation is determined, it is easier to manufacture electrodes by using the highest-mobility direction of sample in an FET-type device.[1]

3.5. Carrier mobility analysis

The carrier mobilities of graphene, BP, and MoS_2 are calculated according to[1]

$$\frac{1}{m_{\mathrm{e}}^*} = \frac{1}{h^2}\frac{\partial^2 E(k)}{\partial k^2}, \tag{2}$$

$$m_{\mathrm{d}}^* = \sqrt{m_x^* m_y^*}, \tag{3}$$

$$\mu_{2\mathrm{D}} = \frac{eh^3 C_{2\mathrm{D}}}{k_{\mathrm{B}} T m_{\mathrm{e}}^* m_{\mathrm{d}}^* \left(E_1^i\right)^2}, \tag{4}$$

where m_x^* and m_y^* are the effective masses of CBM or VBM in two different directions. m_{d}^* is the average effective mass. m_{e}^* is the effective mass in the transport direction. h is the Planck constant, k is the wave vector, and $E(k)$ is the energy. E_1 is the deformation potential. k_{B} is the Boltzmann constant. $C_{2\mathrm{D}}$ is the stretching modulus of the crystal for simulating the lattice distortion activated by strain. The temperature T used for the mobility calculations is 300 K. The results are listed in Table 2, where m_0 is the free electron mass.

From Table 2, we can see that the calculated average effective masses of electrons and holes in graphene are $0.13m_0$ and $0.11m_0$, which are the smallest among graphene, BP, and MoS_2 due to the Dirac point. Graphene has been used to enhance the performance of various energy conversion and storage devices by taking advantage of the zero-band-gap character.[6] The effective masses along x (X–S) direction are significantly larger than those along y (X–U) direction for the calculated BP layers. For example, the effective hole mass of monolayer BP is $5.89m_0$ along the X–S direction and $0.23m_0$ along the X–U direction. The effective electron masses of monolayer BP also have a similar behavior. Effective masses show that the in-plane anisotropic behavior of BP is stronger than that of MoS_2. The electron mobility of BP and MoS_2 from monolayer to five-layer increases, when the effective masses are decreased. The hole effective masses along X–S of BP and along K–H of MoS_2 from the monolayer to the bilayer decrease sharply.[14] This phenomenon proves that BP and MoS_2 have a strongly layer-dependent evolution. Among graphene, BP, and MoS_2, graphene has the highest carrier mobility due to its very low carrier effective masses and deformation potential constant. The calculated hole and electron carrier mobilities of graphene are 4.82×10^4 $\mathrm{cm^2 \cdot V^{-1} \cdot s^{-1}}$ and 5.27×10^4 $\mathrm{cm^2 \cdot V^{-1} \cdot s^{-1}}$, which are smaller than 2×10^5 $\mathrm{cm^2 \cdot V^{-1} \cdot s^{-1}}$.[21] This happens because

Table 2. Predicted carrier mobilities of graphene, BP, and MoS_2.

	Carrier type	N_{L}	m_x^*/m_0	m_y^*/m_0	m_{d}^*/m_0	E_1/eV	$C_{2\mathrm{D}}$/J·m^{-2}	$\mu_{2\mathrm{D}}/10^2$ cm^2·V^{-1}·s^{-1}
Graphene	e	1	0.09	0.18	0.13	2.16	496.5	482.4
	h	1	0.07	0.16	0.11	2.24	496.5	527.5
BP	e	1	1.2	0.25	0.55	4.32	67.8	0.92
		2	1.22	0.28	0.44	5.15	104.32	1.55
		3	1.28	0.26	0.4	6.36	156.24	1.84
		4	1.3	0.25	0.34	7.03	277.96	3.72
		5	1.32	0.26	0.33	7.50	364.31	4.54
	h	1	5.89	0.23	1.16	0.23	67.8	153.65
		2	2.3	0.21	0.69	2.01	104.32	6.5
		3	1.91	0.21	0.63	2.35	156.24	8.59
		4	1.13	0.2	0.47	3.12	277.96	13.67
		5	0.97	0.2	0.44	3.56	364.31	15.14
MoS_2	e	1	0.65	0.5	0.57	8.30	140.6	0.48
		2	0.63	0.6	0.61	9.50	335.1	0.76
		3	0.63	0.78	0.7	9.56	396.5	0.67
		4	0.63	0.79	0.71	9.68	430.6	0.70
		5	0.62	0.84	0.72	10.2	573.2	0.81
	h	1	1.63	0.7	1.07	3.02	140.6	1.93
		2	1.23	0.71	0.93	4.73	332.1	2.00
		3	1.01	0.71	0.85	4.92	396.5	2.11
		4	0.94	0.69	0.81	5.24	430.6	2.09
		5	0.82	0.68	0.75	5.62	573.2	2.57

of the limited number of graphene structures that we have built. The effective masses of monolayer graphene decrease and the stretching moduli increase, when the number of carbon atoms is increased. In this paper, for monolayer BP, it is important to note that hole carrier mobility is 1.5×10^4 $cm^2 \cdot V^{-1} \cdot s^{-1}$ duo to the extremely small deformation potential. This is larger than the carrier mobility of 2.6×10^4 $cm^2 \cdot V^{-1} \cdot s^{-1}$ in a previous paper.[6] For MoS_2, the actual measured carrier mobilities of bulk, monolayer, and multilayer of MoS_2 are 50–200 $cm^2 \cdot V^{-1} \cdot s^{-1}$, 200 $cm^2 \cdot V^{-1} \cdot s^{-1}$, and 7×10^2 $cm^2 \cdot V^{-1} \cdot s^{-1}$ at room temperature, respectively.[22,23] The calculated values are in good agreement with the actual measured values. The hole carrier mobilities of graphene, BP, and MoS_2 are larger than the electron carrier mobilities. For BP and MoS_2, the carrier mobility increases when the number of layers is increased. Graphene has the highest carrier mobility.

3.6. Loss function analysis

Figure 6 shows the loss functions of monolayer graphene, BP, and MoS_2. Graphene has three sharp loss peaks, which are located at 4.77 eV, 15.90 eV, and 18.40 eV. BP has only one sharp loss peak, which is located at 9.71 eV. However, MoS_2 has a wide range of loss peak from 6.60 eV to 17.35 eV. The sharp loss peak suggesting that the optical storage efficiency can be enhanced easily. Among monolayer graphene, BP, and MoS_2, BP has superior optical storage efficiency.

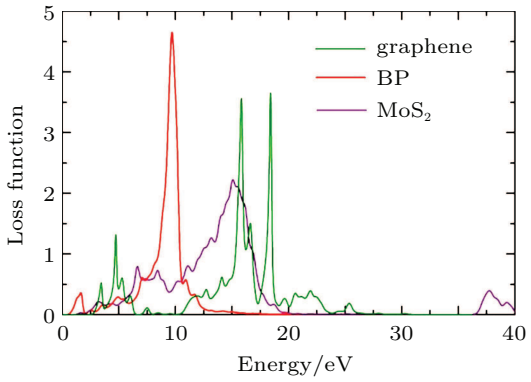


Fig. 6. (color online) The loss functions of monolayer graphene, BP, and MoS_2.

4. Conclusion

In brief, by first-principles calculation, we have shown that the band gaps of BP and MoS_2 are strongly dependent on the number of layers. The band gap of MoS_2 is 1.002–1.806 eV, and that of BP is 0.511–1.227 eV, from monolayer to five-layer. The graphene is a zero-band-gap semiconductor. The relationship of the layers and the band gap is built to predict the band gap of few-layer BP and MoS_2. The absorption shows an explicit anisotropy for light polarized in (1 0 0) and (0 0 1) directions of graphene, BP, and MoS_2. This behavior may be readily detected in spectroscopic measurements and exploited for optoelectronic applications. Graphene, monolayer BP, and MoS_2 have high carrier mobility. The decreasing trend for carrier effective masses with increasing number of layers suggests a higher mobility for multilayer BP compared to monolayer BP. Among graphene, BP, and MoS_2, BP has superior optical storage efficiency, which can be used in optical storage devices. These results suggest that graphene, BP, and MoS_2 have abundant opportunities for a plethora of new electronic applications.

References

[1] Qiao J S, Kong X H, Hu Z X, Yang F and Ji W 2014 *Nat. Commun.* **5** 5475
[2] Cai Y Q, Zhang G and Zhang Y W 2014 *Sci. Rep-Uk* **4** 6677
[3] Takahashi T, Tokailin H, Suzuki S, Sagawa T and Shirotani I 1984 *Phys. Rev. B* **29** 1105
[4] Rudenko A N and Katsnelson M I 2014 *Phys. Rev. B* **89** 201408
[5] Wang C C, Zhan Y and Wang Z Y 2018 *Chemistryselect* **3** 1713
[6] Hu J S, Ji G P, Ma X G, He H and Huang C Y 2018 *Appl. Surf. Sci.* **440** 35
[7] Phuc H V, Hieu N N, Hoi B D, Hieu N V, Thu T V, Hung N M, Ilyasov V V, Poklonski N A and Nguyen C V 2018 *J. Electron. Mater* **47** 730
[8] Jia W L, Zhou M, Wang X M and Ji W L 2018 *Acta Phys. Sin.* **67** 107102
[9] Menezes M G and Capaz R B 2018 *Comp. Mater Sci.* **143** 411
[10] Phuc H V, Ilyasov V V, Hieu N N and Nguyen C V 2018 *Vacuum* **149** 231
[11] Carlsson J M and Scheffler M 2006 *Phys. Rev. Lett.* **96** 046806
[12] Huang G Q and Xing Z W 2015 *J. Phys-Condens Mat.* **27** 175006
[13] Cartz L, Srinivasa S R, Riedner R J, Jorgensen J D and Worlton T G 1979 *J. Chem. Phys.* **71** 1718
[14] Scalise E, Houssa M, Pourtois G, Afanas'ev V V and Stesmans A 2014 *Physica E* **56** 416
[15] Cao J, Zhou J, Zhang Y and Liu X 2018 *Microelectronic Engineering* **190** 63
[16] Wei Q and Peng X H 2014 *Appl. Phys. Lett.* **104** 372
[17] Zhang Z, Zhao Y and Ouyang G 2017 *The Journal of Physical Chemistry C* **121** 19296
[18] Zhu J, Park H, Chen J Y, Gu X K, Zhang H, Karthikeyan S, Wendel N, Campbell S A, Dawber M, Du X, Li M, Wang J P, Yang R G and Wang X J 2016 *Adv. Electron Mater* **2** 1600040
[19] Jin W C, Yeh P C, Zaki N, Zhang D T, Sadowski J T, Al-Mahboob A, van der Zande A M, Chenet D A, Dadap J I, Herman I P, Sutter P, Hone J and Osgood R M 2013 *Phys. Rev. Lett.* **111** 106801
[20] L Kane C and J Mele E 2005 *Phys. Rev. Lett.* **95** 226801
[21] Bolotin K I, Sikes K J, Jiang Z, Klima M, Fudenberg G, Hone J, Kim P and Stormer H L 2008 *Solid State Commun.* **146** 351
[22] Das S, Chen H Y, Penumatcha A V and Appenzeller J 2013 *Nano Lett.* **13** 100
[23] Kim S, Konar A, Hwang W S, Lee J H, Lee J, Yang J, Jung C, Kim H, Yoo J B, Choi J Y, Jin Y W, Lee S Y, Jena D, Choi W and Kim K 2012 *Nat. Commun.* **3** 1038